Experimental Research on Machinability of Ti2AlNb Intermetallic Alloy

He Linjiang, *Su Honghua* *, *Xu Jiuhua*, *Zhang Liang*, *Bai Bing*

College of Mechanical and Electrical Engineering, Nanjing University of Aeronautics and Astronautics, Nanjing 210016, P. R. China

(Received 22 June 2016; revised 28 August 2016; accepted 31 August 2016)

Abstract: Ti2AlNb intermetallic alloy is a newly developed high-temperature resistant structural material due to its excellent material and mechanical properties, which also make it to be one of the most difficult-to-cut materials. In order to study the machinability of Ti2AlNb alloy, a series of turning experiments of Ti2AlNb alloy with varying cutting speed and feed rate using coated carbide tools are carried out. The results associated with cutting forces, cutting temperature and tool wear are presented and discussed. Moreover, the cutting performance of Ti2AlNb alloy is evaluated in comparison with that of most commonly used Ti6Al4V and Inconel 718 alloys in terms of the cutting forces and cutting temperature. The comparison results show that there is a correlation between the machinability and the mechanical properties of work material properties. Additionally, considering material removal rate and tool life, the optimized machining parameters for cutting Ti2AlNb alloys using coated carbide tools are recommended.

Key words: intermetallic alloy; machinability; cutting force; cutting temperature; tool wear

CLC number: TG506.1 **Document code**: A **Article ID**: 1005-1120(2017)05-0487-09

0 Introduction

In the past two decades, considerable efforts have been made to develop several kinds of light-weight high-temperature resistant material to replace the nickel-based super alloy for thermally and mechanically stressed components in aerospace and automotive engines[1, 2]. Recently, a new class of titanium intermetallic alloys, based on the orthorhombic TiAl (O) phase, has been attaining great attention due to their high strength/weight ratio, high stiffness and excellent specific strength retention at elevated temperature. However, the application is still limited due to the low ductility and low fracture toughness of these alloys. By adding elements of Cr or Mn into the TiAl-based alloy to increase ductility, and Nb to improve strength and oxidation, Ti_2AlNb intermetallic alloy is assumed to own the best balance of tensile, creep, strength-to-weight ratio, fracture toughness properties[3, 4]. However, such properties along with the low thermal conductivity, high chemical reactivity with tool materials, and strong tendency to hardening, make Ti2AlNb intermetallic alloy to be one of the most difficult-to-cut materials[5-7]. At present, most of the work on Ti2AlNb alloy focus on the material composition and structural properties, while the research of the machinability is insufficient[8-11]. In order to provide the guidance for cutting parameters selection to improve the machining performance of Ti2AlNb alloy, a deeper knowledge of its machinability is required.

This paper described a series of turning experiments campaign aimed at the machinability of Ti2AlNb intermetallic alloy with varying cutting speed and feed rate. The coated carbide tools are adopted during the turning experiments. Experi-

* Corresponding author, E-mail address: shh@nuaa.edu.cn.

How to cite this article: He Linjiang, Su Honghua, Xu Jiuhua, et al. Experimental research on machinability of Ti2AlNb intermetallic alloy[J]. Trans. Nanjing Univ. Aero. Astro., 2017,34(5):487-495.
http://dx.doi.org/10.16356/j.1005-1120.2017.05.487

mental results are presented and discussed in terms of cutting forces, cutting temperature and tool wear modes. Furthermore, the cutting performance of Ti2AlNb alloy is evaluated in comparison to that of most commonly used Ti6Al4V and Inconel 718 alloys in terms of the cutting forces and cutting temperature.

1 Material and Experiment Procedure

1.1 Workpiece material

The Ti2AlNb intermetallic alloy with diameter of 150 mm is used as workpiece material. The main chemical compositions are listed in Table 1. A microstructural observation by optical scope (Leica DM6M) on the material reveals that small lamellar O phase and α_2 phase are uniform distributed within the B_2 matrix, as shown in Fig. 1. In order to investigate the machinability of Ti2AlNb comparatively, the commonly used Ti6Al4V and Inconel 718 alloys are employed during machining experiments. The properties of Ti2AlNb intermetallic alloy, Ti6Al4V and Inconel 718 alloys are shown in Table 2[12-14]. Fig. 2 shows the dynamic flow stress curves of three alloys with varied temperature, which are plotted based on the dynamic constitutive model[15-17]. It can be seen that the flow stress of Ti2AlNb alloy is lower than Inconel 718 alloy but higher than Ti6Al4V alloy at room temperature. As temperature increases, the flow stress of Ti2AlNb alloy remains almost constant under 600 ℃, while the flow stresses of Inconel 718 and Ti6Al4V alloys decrease rapidly.

Table 1 Main chemical composition of Ti2AlNb (wt%)

Al	Nb	Mo	O	H	N	Ti
22—25	20—30	2—3	≤0.1	≤0.01	≤0.1	Bal

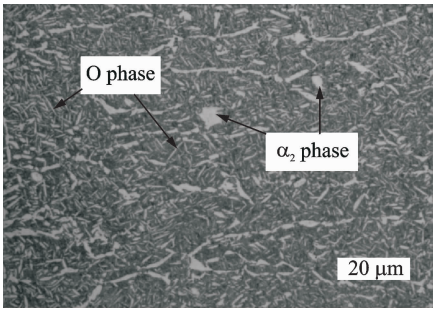

Fig. 1 Ti2AlNb microstructure

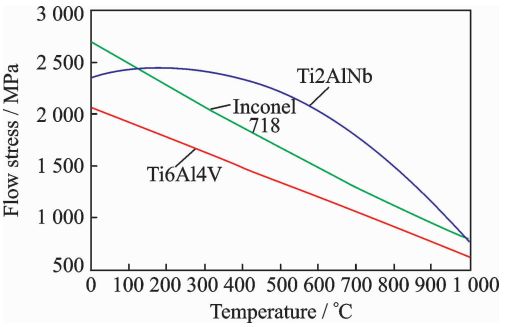

Fig. 2 Dynamic flow stresses versus temperature of Ti2AlNb, Inconel 718 and Ti6Al4V alloy at strain rate 10 000 s^{-1}

1.2 Cutting tools and tool wear measurement

The single layer TiAlN (PVD) coated carbide inserts are employed in the turning tests. The parameters of the cutting tools are listed in Table 3. Tools are periodically examined in order to measure the tool wear at different cutting time by an optical microscope (KH7700), which is equipped with a high-resolution camera for image acquisition. Tool rejection or failure is determined based on the following criteria: Average flank wear $VB = 0.2$ mm, maximum flank wear $VB_{max} = 0.4$ mm, and chipping or flaking of the cutting edge. The tests are performed until the tool failure criterion is reached.

Table 2 Main mechanical properties of Ti2AlNb, Ti6Al4V and Inconel 718[12-14]

Material	Density/ ($g \cdot cm^{-3}$)	Yield strength / MPa	Elastic modulus/ GPa	Thermal conductivity/ ($W \cdot m^{-1} \cdot K^{-1}$)	Specific heat capacity/ ($J \cdot kg^{-1} \cdot K^{-1}$)	Linear expansion coefficient/ ($10^{-6} \cdot K^{-1}$)
Ti2AlNb	5.35	1 030	120	6.3	417	8.22
Ti6Al4V	4.43	950	113.8	6.7	423	8.53
Inconel 718	8.24	1 260	199	13.4	467	11.8

Table 3 Parameters of cutting tools

Parameter	Value
Corner radius r_ε /mm	0.4
Cutting edge roundness r_n /μm	(20±3)
Rake angle γ_0/(°)	5
Clearance angle α_0/(°)	7
Tool cutting edge angle κ_r/(°)	95

1.3 Machining test

All of the machining tests are carried out on a SK-50P CNC turning machine, as shown in Fig. 3. A Kistler 9272 dynamometer and a 5019A charge amplifier are used to measure the three-component cutting forces (F_x—the radial force, F_y—the feed force and F_z—the cutting force). The force measurements are sampled and digitally low-pass filtered to eliminate the high-frequency components resulting from the machine tool dynamics and electrical noise, as shown in Fig. 4.

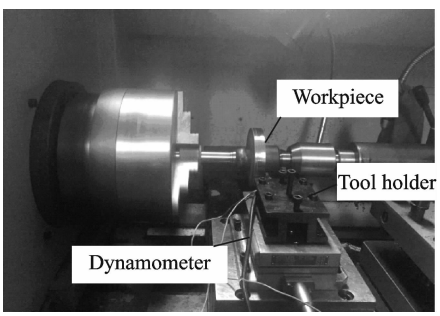

Fig. 3 Experimental setup

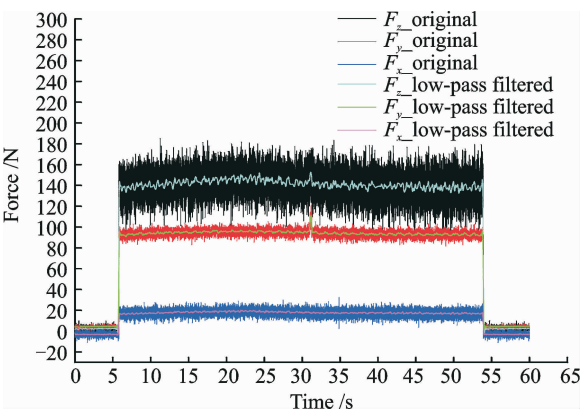

Fig. 4 Force signal curves (v = 50 m/min, f = 0.1 mm/rev, a_p = 0.5 mm)

In addition, the tool-workpiece natural thermocouple is employed to measure the cutting temperature. The hot junction of the thermocouple is formed when the tool is cutting the workpiece material. The electromotive force signals between the hot junction and cold junction of the thermocouple are recorded using NI USB-6211 dynamic signal acquisition system. The original and low-pass filtered electromotive force signals are shown in Fig. 5. Then the cutting temperature can be calculated after the calibration of the electromotive force using a special calibration system, as illustrated by Bian[18]. The calibration curves of Ti6Al4V/Ti2AlNb/Inconel 718 alloy-tool thermocouple are shown in Fig. 6.

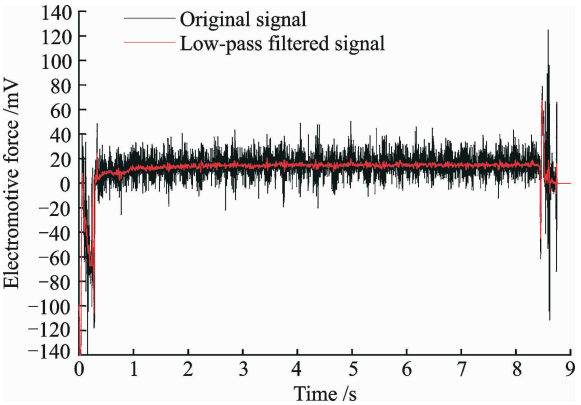

Fig. 5 Thermal electromotive force signal (v = 50 m/min, f = 0.1 mm/rev, a_p = 0.5 mm)

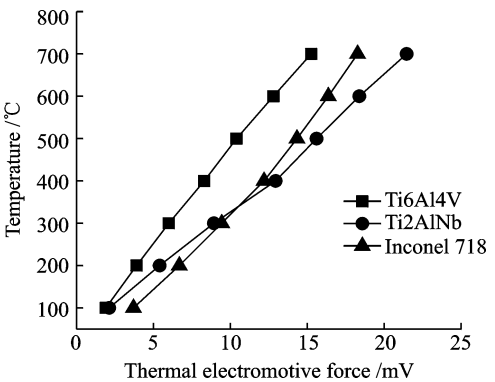

Fig. 6 Calibration curves of material-tool thermocouple

1.4 Experimental parameters and cutting conditions

In order to study the machinability of Ti2AlNb alloy, depth of cut a_p is kept constant as 0.5 mm, while the cutting speed v and feed rate f are assumed as the independent input variables. The cutting speed varies from 40 m/min to 80 m/min, and the feed rate varies from 0.06 mm/rev to 0.12 mm/rev, as shown in Table 4. The turning operations are performed with 5% emulsion of oil in water.

Table 4 Experimental parameters

Parameter	Value
Cutting speed v/(m · min^{-1})	40, 50, 60, 70, 80
Feed rate f/(mm · rev^{-1})	0.06, 0.08, 0.1, 0.12
Depth of cut a_p/mm	0.5

2 Results and Discussion

2.1 Effect of cutting speed and feed rate on the cutting force and cutting temperature of Ti2AlNb alloy

Cutting force and cutting temperature strongly affect the tool life, surface quality and the power consumption, which are often used to evaluate the cutting performance of workpiece[18]. Fig. 7 shows the variation of cutting temperature of Ti2AlNb alloy with various cutting speeds and feed rates at a constant cutting depth of 0.5 mm. It is shown clearly that with the increasing of cutting speed and feed rate, the cutting temperature increases rapidly. For instance, the cutting temperature increases from 470 ℃ for v=40 m/min to 565 ℃ for v=80 m/min at the same feed rate f=0.1 mm/rev. It is illustrated that when cutting at higher speed, the strain rate in the shear zone is expected to be higher, thus more heat energy will be generated[19]. Moreover, the time for heat dissipation decreases with the increasing cutting speed. Thus the heat generated will accumulate at the cutting zone and result in a higher temperature at the tool-chip interface. However, the elevated higher temperature still does not reach the transition point that the flow stress of Ti2AlNb alloy becomes soften because of the reinforcement of O phase on the material microstructure, but will bring a big challenge to the cutting tool materials. At such high temperature, most tool materials will lose their hardness and strength to cutting materials functionally.

Fig. 8 shows that the feed force decreases rapidly as cutting speed increases, while the cutting force almost keeps constant. The magnitudes of cutting force and feed force both increase with increasing feed rate. For instance, the feed force decreases from 118 N to 85 N as the cutting speed

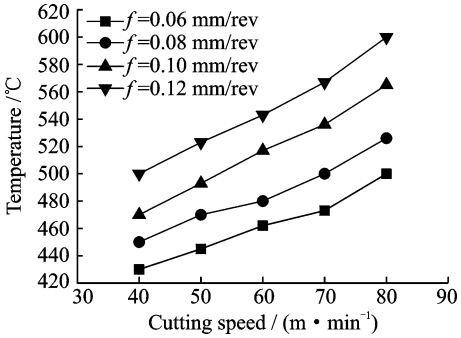

Fig. 7 Variation of cutting temperature with cutting speed and feed rate

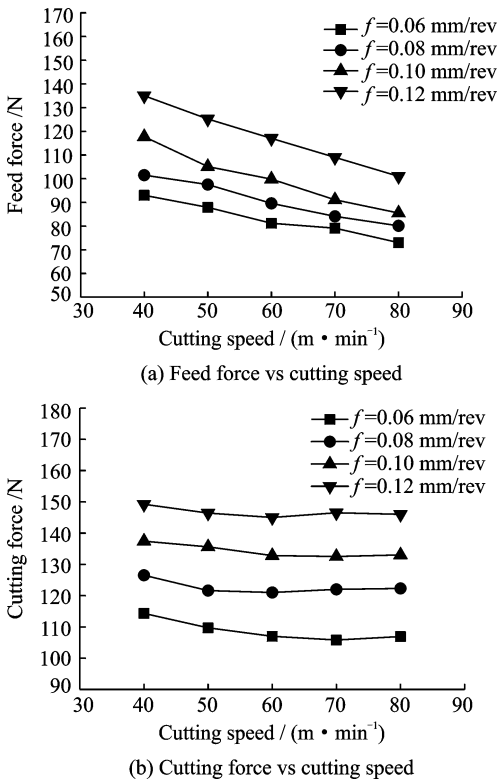

Fig. 8 Variation of cutting forces varying with cutting speed and feed rate at depth of cut a_p=0.5 mm

increases from 40 m/min to 80 m/min at the feed rate of 0.1 mm/rev, while the cutting force keeps almost constant of 135 N. It is reported that the friction coefficient has a significant effect on the feed force and the friction coefficient between tool and work material decreases as the cutting speed increases[20]. Therefore, the feed force decreases almost linearly with increasing cutting speed. Furthermore, as the cutting speed increases, the higher temperature generated can not lead to the material soften a lot at cutting zone because of the material's high strength retention property with the coupling of machining hardening effect of

higher strain and strain rate. This is the reason that the cutting force almost keeps constant with increasing cutting speed. Thus, the cutting speed at a medium range of 40—60 m/min and feed rate at a medium range of 0.08—0.1 mm/rev for machining Ti2AlNb alloys using coated carbide tools is recommended in order to obtain relatively low cutting force and high material remove rate.

2.2 Tool wear and failure modes

Tool wear can directly reflect the cutting condition at the cutting zone and affect the optimization results of cutting parameters[21]. Therefore, tool wear and failure modes are also applied to evaluate the machinability of work material. Fig. 9 illustrates the example of coated carbide inserts tool wear process for the case $v=50$ m/min and $f=0.1$ mm/rev. The flank tool wear and nose wear are relatively uniform at the beginning of the turning process. Then non-uniform wear at the flank face is found to dominate under the whole cutting process. The wear rate on the flank face is observed to be much greater than that on the rake face of the tools. It is assumed that the flank face endures extremely friction and high cutting pressure condition from the machined surface due to low elastic modulus and elastic/plastic deformation of work material. Furthermore, the adhesion of Ti2AlNb alloy material on the flank face can be observed in Fig. 9 (i), which suggests that there exists high bonding strength between coating and the adhered material. The coating will be worn out or coating delamination will occur soon after the adhered or welded work material is hit and squashed by the chip or the machined surface, as illustrated in Fig. 10. As the coating is removed so quickly, the tool substrate is exposed to the freshly generated underside of the chip and transient surface of the work directly. The high temperature and high frequency cutting load resulted from serrated chip will lead to the initiation of chipping and finally to the breakage of carbide at the cutting edge, as can be seen in Fig. 9 (e).

The flank wear curves of tools under different cutting conditions are shown in Fig. 11. It can be found that the tool wear rate increases rapidly in the initial stage and in the steady stage, the tool wear increases smoothly. However, in the last stage, the tool wear increases dramatically again. The flank wear and tool life are significantly influenced by the cutting speed and feed rate. For instance, tool life decreases rapidly from 18.5 min to less than 2.5 min as cutting speed increases from 40 m/min to 80 m/min. The tool life in-

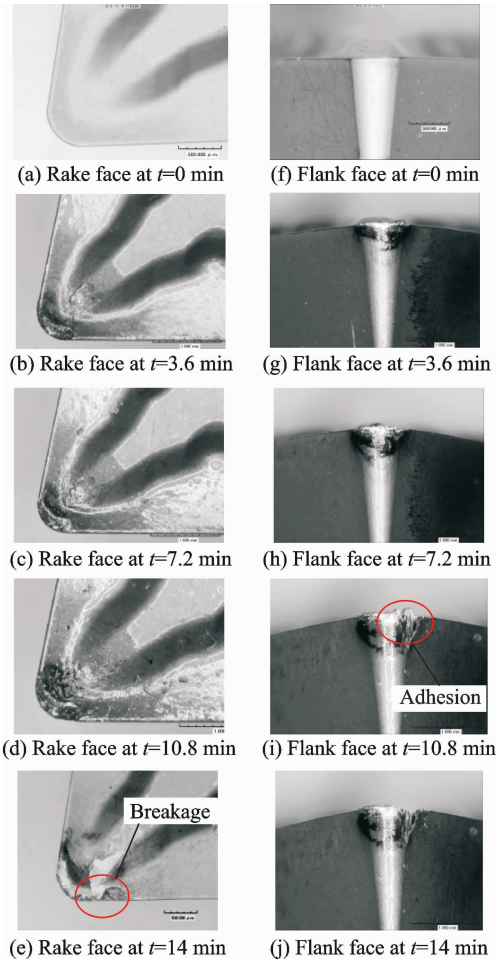

Fig. 9 Typical tool wear process ($v=50$ m/min, $f=0.1$ mm/rev)

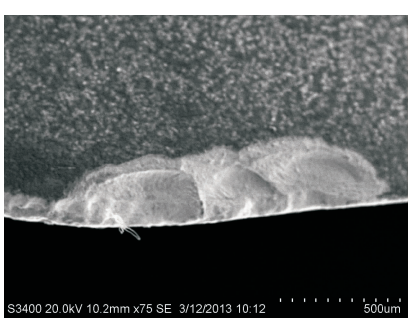

Fig. 10 Coating delamination on rake face ($t=12$ min)

creases from 9.5 min to 16.5 min as the feed rate reduces from 0.12 mm/rev to 0.06 mm/rev. Furthermore, when the cutting speed $v \geqslant 60$ m/min, there hardly exists the smooth process of tool wear, which indicates that the tool wear rate is extremely high in the whole cutting process. It can be explained that an increase in cutting speed and feed rate causes a greater increment in cutting temperature at the cutting edge of the tools, resulting in their strength loss of the tool edge and then plastic deformation[22-23]. Reducing cutting speed and feed rate can significantly improve the tool life. However, this corresponds to low cutting efficiency.

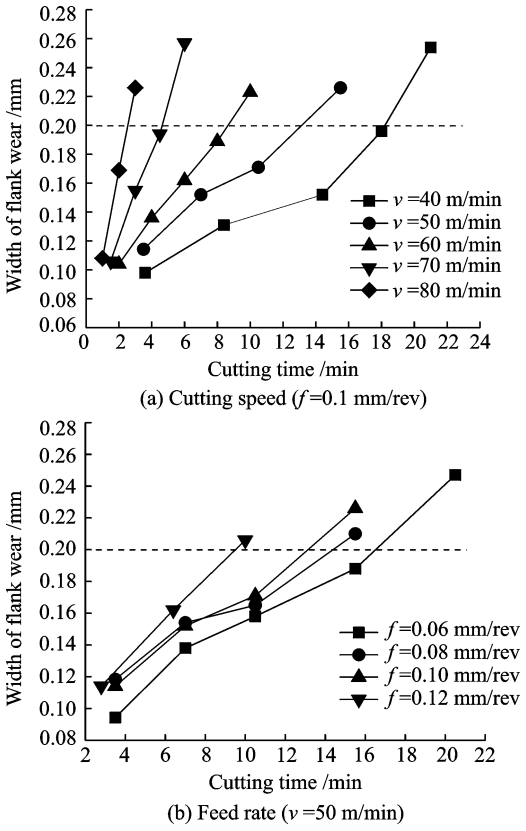

Fig. 11 Flank wear curves of tools at different cutting conditions

Fig. 12 shows the total material removal volume at different cutting parameters when the cutting tools reach the failure criteria. The total material removal volume is calculated from the following expression

$$V \approx 1\,000 v f a_p T \tag{1}$$

It can be seen that with increasing cutting speed, the total material removal volume decreases significantly. Furthermore, as feed rate increases from 0.06 mm/rev to 0.1 mm/rev, the total material removal volume increases from 24 750 mm^3 to 32 750 mm^3, and then decreases to 28 200 mm^3 when feed rate increases to 0.12 mm/rev. It can be indicated that cutting speed in the range of 40—50 m/min and feed rate in the range of 0.08—0.1 mm/rev obtain optimum cutting parameters in considering of material removal rate and tool life.

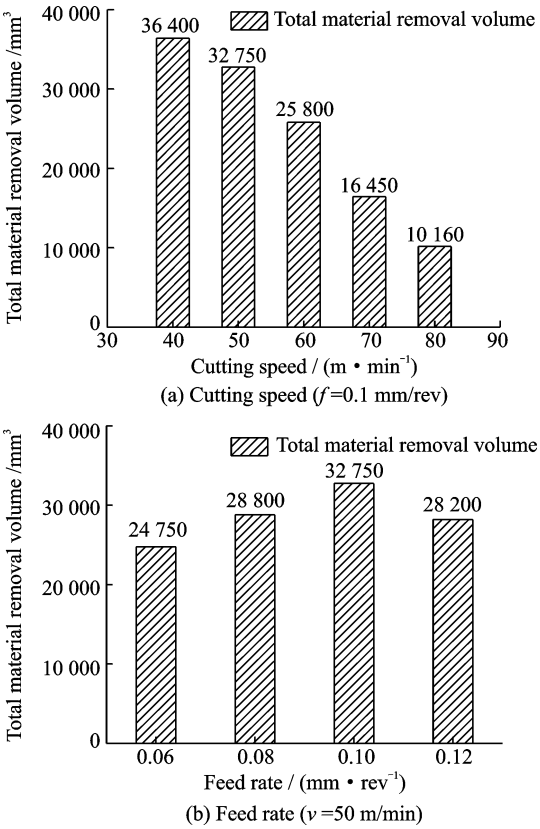

Fig. 12 Total material removal volume at different cutting parameters

2.3 Evaluation of cutting performance of Ti2AlNb alloy

In order to evaluate the cutting performance of Ti2AlNb alloy, the cutting force and cutting temperature are measured and subsequently compared with that of most commonly used Ti6Al4V alloy and Inconel 718 alloy. Fig. 13 demonstrates that the cutting force and the cutting temperature values correlate well with the mechanical properties of the alloys. Lower cutting force values are obtained for Ti6Al4V alloy whereas higher values for the Ti2AlNb alloy and Inconel 718. For instance, at the cutting speed $v = 50$ m/min, the

cutting force of Ti6Al4V, Ti2AlNb and Inconel 718 alloys are 100, 134, and 200 N, respectively and the cutting temperature is 430, 493, and 580 ℃, respectively. Furthermore, as cutting speed increases, the cutting temperature of Inconel 718 alloy increases more rapidly than Ti2AlNb alloy, which will induce the flow stress of Inconel 718 alloy soften gradually. Thus the cutting force of Inconel 718 alloy decreases, but still higher than that of Ti2AlNb. As for Ti6Al4V alloy, cutting force remains almost constant at cutting speed $v \leqslant 60$ m/min, then decreases rapidly as cutting speed increases at $v > 60$ m/min. It can be explained that when the cutting speed is under 60 m/min, the Ti6Al4V alloy remains high strength due to its cutting temperature does not reach the transition point that material flow stress becomes soften. However, when the cutting speed is above 60 m/min, the cutting temperature is up to 460 ℃, and the thermal soften effect is higher than strain hardening effect, thus resulting in the decrease of material flow stress[24], while Ti2AlNb alloy still remains high strength due to the reinforcements of O phase on the material microstructure, which induces the excellent high temperature resistant and mechanical properties. Therefore, it indicates that the machinability of Ti2AlNb alloy is better than that of Inconel 718 alloy, but worse than that of Ti6Al4V alloy. Therefore, as Ti2AlNb alloy is expected to replace the Inconel 718 alloy as thermal and mechanical stressed components, it is very promising and necessary to study the machinability of Ti2AlNb alloy and optimize the cutting parameters to improve the cutting process.

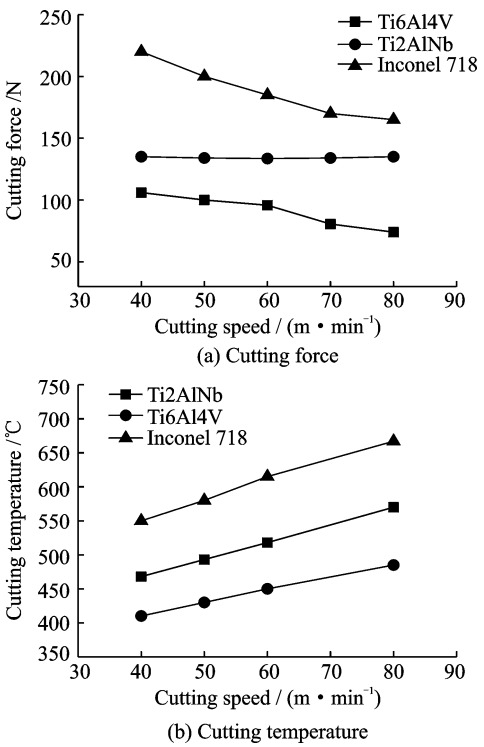

Fig. 13 Comparison results of Ti2AlNb, Ti6Al4V and Inconel 718 at feed rate $f = 0.1$ mm/rev and depth of cut $a_p = 0.5$ mm

3 Conclusions

Based on the cutting performance and experimental results for analyzing the influence of cutting parameters on the machinability characteristics of Ti2AlNb alloy and the comparison results with Ti6Al4V and Inconel 718 alloy, the following conclusions are drawn:

(1) The feed force decreases by 42% as cutting speed increases from 40 m/min to 80 m/min, while the cutting force almost keeps constant at the same feed rate. The cutting temperature increases by 12.7% as cutting speed increases from 40 m/min to 80 m/min. The cutting force and cutting temperature almost keep linear dependent on feed rate.

(2) Tool life is heavily affected by the cutting speed and feed rate, and the cutting speed is the predominant factor. When the cutting speed exceeds 50 m/min, the tool wear rate increases dramatically and the tool life decreases to even less 5 min.

(3) The main type of tool wear is flank wear and breakage of cutting edge, where high temperature and adhesion of workpiece material are assumed to be responsible for the failure of cutting tools.

(4) The recommended machining conditions for Ti2AlNb intermetallic alloy using coated carbide tools will be the selection of cutting speed range (40—50 m/min) with feed rate (0.08—0.1 mm/rev) in terms of material removal rate and the tool life.

(5) The machinability rate of Ti2AlNb intermetallic alloy can be worse than Ti6Al4V alloy by approximately 25% and better than Inconel 718 alloy by 33%, comparing the cutting force and cutting temperature of the three alloys, which can be deduced that the machinability correlates well with the mechanical properties of the alloys.

Acknowledgement

This work was supported by the National Natural Science Foundation of China (51475233).

References:

[1] HAGIWARA M, EMURA S, ARAOKA A, et al. The effect of lamellar morphology on tensile and high-cycle fatigue behavior of orthorhombic Ti-22Al-27Nb alloy [J]. Metallurgical and Materials Transactions A, 2004, 35(7):2161-2170.

[2] MURALEEDHARAN K, NANDY T K, BANERJEE D. Phase stability and ordering behaviour of the O phase in Ti2AlNb alloys [J]. Intermetallics, 1995, 3(3): 187-199.

[3] AUSTIN C M. Current status of Gamma titanium aluminides for aerospace applications [J]. Current Opinion in Solid State Materials Science, 1999, 4(3): 239-242.

[4] LORIA E A. Gamma titanium alminides as a prospective structural materials [J]. Intermetallics, 2000, 8 (9/10/11): 1339-1345.

[5] ASPINWALL D K, DEWES R C. The machining of γ-TiAl intermetallic alloys [J]. Annals of the CIRP, 2005, 54(1): 99-104.

[6] MANTLE A L, ASPINWALL D K. Surface integrity of a high speed milled Gamma titanium aluminide [J]. Journal of Materials Processing Technology, 2001, 118(1/2/3): 143-150.

[7] SHARMAN A R C, ASPINWALL D K, DEWES R C, et al. Workpiece surface integrity considerations when finish turning Gamma titanium aluminide [J]. Wear, 2001, 249(5/6): 473-481.

[8] QUAST J P, BOEHLERT C J. Comparison of the microstructure tensile and creep behavior for Ti-24Al-17Nb-0.66Mo and Ti-24Al-17Nb-2.3Mo alloys [J]. Metallurgical and Materials Transactions A, 2007, 38(3):529-536.

[9] CHENG T T, WILLIS M R. Effects of major alloying additions on the microstructure and mechanical properties of γ-TiAl[J]. Interemtallics, 1999, 7(1): 89-99.

[10] GERMANN L, BANERJEE D, GUEDOU J Y, et al. Effect of composition on the mechanical properties of newly developed Ti2AlNb-based titanium aluminide [J]. Intermetallics, 2005, 13(9):920-924.

[11] ZHANG Q C, CHEN M H, WANG H, et al. Thermal deformation behavior and mechanism of intermetallic alloy Ti2AlNb [J]. Transactions of Nonferrous Metals Society of China, 2016, 26(3):722-728.

[12] JAFFERY S I, MATIVENGA P T. Assessment of the machinability of Ti-6Al-4V alloy using the wear map approach[J]. International Journal of Advanced Manufacturing Technology, 2009, 40: 687-696.

[13] SHI Q. Analysis on surface integrity during high speed milling for new damage-tolerant titanium alloy [J]. Transactions of Nanjing University of Aeronautics & Astronautics, 2012, 29(3):222-226.

[13] MA X D, XU J H, DING W F, et al. Wear behavior of Ti(N, C)-Al_2O_3 coated cemented carbide tools during milling Ti2AlNb based alloy[J]. Key Engineering Materials, 2014, 589/590:361-365.

[14] THAKUR D G, RAMAMOORTHY B, VIJAYARAGHAVAN L. Study on the machinability characteristics of superalloy Inconel 718 during high speed turning[J]. Materials and Design, 2009, 30(5):1718-1725.

[15] KLOCKE F, LUNG D. Inverse identification of the constitutive equation of Inconel 718 and AISI 1045 from FE machining simulations [C]// 14th CIRP CMMO. Turin, Italy: Procedia CIRP, 2013, 8: 212-217.

[16] MADALINA C, DOMINIQUE C, GIROT F. A new material model for 2D numerical simulation of serrated chip formation when machining titanium alloy Ti-6Al4V [J]. International Journal of Machine Tools & Manufacture, 2008, 48:275-288.

[17] WANG Wei. Research on the high temperature constitutive equations of Ti2AlNb based intermetallic compound [D]. Nanjing: Nanjing University of Aeronautics and Astronautics, 2014: 30-48. (in Chinese)

[18] BIAN Weiliang. Experimental study on turning of titaninum ,atrix composites [D]. Nanjing: Nanjing University of Aeronautics and Astronautics, 2012: 43-47. (in Chinese)

[19] KONIG W, FRITSCH R, KAMMERMEIER D. Physically vapor deposited coatings on tools: Performance and wear phenomena[J]. Surface and Coatings Technology, 1991, 49(1/2/3):316-324.

[20] TROY D M. Effects of friction and cutting speed on cutting force [C]// Proceedings of ASME Congress, New York, NY:[s. n.], 2001:11-16.

[21] XUE C, CHEN W Y. Adhering layer formation and its effect on the wear of coated carbide tools during turning of a nickel-based alloy [J]. Wear, 2011, 270 (11/12): 895-902.

[22] JAWAID A, SHARIF S, KOKSAL S. Evaluation of wear mechanisms of coated carbide tools when face milling titanium alloy [J]. Journal of Materials Processing Technology, 2000, 99(1/2/3): 266-274.

[23] QI B Y. Effect of cooling/lubrication medium on machinability of Ti6Al4V [J]. Transactions of Nanjing University of Aeronautics & Astronautics, 2011, 28 (3): 225-230.

[24] PRIARONE P C, RIZZUTI S, ROTELLA G, et al. Tool wear and surface quality in milling of a Gamana-Tial intermetallic [J]. International Journal of Advanced Manufacturing Technology, 2012, 61(1): 25-33.

Mr. **He Linjiang** received his B. S. degree in Mechanical Engineering and Automation from Nanjing University of Aeronautics and Astronautics in 2011. He joined in Nanjing University of Aeronautics and Astronautics for pursuing Ph. D. degree in September 2013. His research is focused on high effective machining of difficult-to-cut materials.

Prof. **Su Honghua** received his Ph. D. degree in Mechanical Engineering from Nanjing University of Aeronautics and Astronautics in 2007. From 2007 to present, he has been a professor of College of Mechanical and Electrical Engineering. His research has focused on high effective machining/grinding technology, Super-abrasive tool technology and high precision machining technology.

Prof. **Xu Jiuhua** received his B. S. and Ph. D. degrees in Mechanical Engineering from Nanjing University of Aeronautics and Astronautics in 1986 and 1992, respectively. From 1992 to present, he has been a full professor of College of Mechanical and Electrical Engineering. His research has focused on high effective machining/grinding technology, Super-abrasive tool technology and high precision machining technology.

Mr. **Zhang Liang** received his B. S. degree in Mechanical Engineering from Hohai University in 2015. From 2015 to present, he has studied in Nanjing University of Aeronautics and Astronautics for M. S. degree. His research has focused on high efficient machining of difficult-to-cut materials.

Mr. **Bai Bing** received his M. S. degree in Mechanical Engineering from Nanjing University of Aeronautics and Astronautics in 2016. His research has focused on modeling of friction behavior in the interface between tool and chips.

(Executive Editor: Xu Chengting)